Available online at www.sciencedirect.com

ScienceDirect

Procedia Engineering 00 (2011) 000–000

Procedia Engineering

www.elsevier.com/locate/procedia

ICM11

Vacuum Oxy-nitrocarburization of Ultra Fine Electrolytic Iron

M.P. Nikolova[a]*, P.S. Danev[a], I.D. Dermendjiev[a], D.D. Gospodinov[a]

[a]*Univerisity of Ruse, 8 Studentska Str., 7017 Ruse, Bulgaria*

Abstract

Samples of Armco iron with electrolytic Fe coating were hardened by vacuum oxy-nitrocarburizing at low temperature. The carbon amount (CO_2) in the nitriding atmosphere (NH_3) was 10 vol. % at a pressure of 8.10^4 Pa and the process time was 7 h. The influence of the structural difference on the depth profile, hardness distribution and X-ray diffraction pattern of the oxy-nitrocarburized specimens were performed. The indicated parameters of the modified surface of electrolyte-precipitated Fe were compared to those of recrystallized at low-temperature and fully annealed in vacuum and oxy-nitrocarburized specimens. The results confirmed formation of γ'- and ε-phases in the compound layer in all samples in different proportions. A significant difference in the phase distribution between the electrolyte-precipitated Fe layer and the substrate was demonstrated due to the ultra fine grained structure of the iron.

Keywords: thermo-chemical treatment; compound zone; diffusion zone; hardness profile; X-ray diffraction

1. Introduction

There are different gaseous ferrite nitrocarburizing methods among which are the low pressure processes in NH_3 + CO_2 mixture atmosphere. The CO_2 containing gas phase has a comparatively high oxygen potential and the oxygen atoms accelerates the $Fe_3(N,C)$ formation [1]. At low pressure conditions oxygen contributes in adherent nitrocarburized layers formation [2]. The structure of the layers depends on process conditions, gas composition and the substrate specific features [3]. It is established that gaseous oxy-nirtrocarburizing (ONC) increases surface hardness and wear resistance, enhances fatigue strength and corrosion resistance of inexpensive non-alloyed or low-alloy steels. The aim of the

* Corresponding author. Tel.: +359888785133

E-mail address: mpnikolova@uni-ruse.bg (M.P. Nikolova)

study is to determinate the structural and hardness differences of vacuum ONC-ed layers formed on metallurgically and galvanically produced iron substrate in NH_3 and CO_2 containing gas phase.

2. Experimental details

Samples of an Armco iron (A-Fe) with thickness about 10 mm and chemical composition ("SPECTRON" quantometer) listed in Table 1 are used as substrates for electrolytic Fe deposition and ONC. Before electroplating, the samples were electrochemically cleaned for 20 - 30 s in 30 % water solution of H_2SO_4 and current density of 100 A/dm^2 in order to improve the adhesion. The electrolytic Fe (E-Fe) coating was obtained in water solution of $FeCl_2.4H_2O$ (30 g/l) acidited by HCl up to pH = 1 – 1,2. The electrolysis is carried out at 80 ± 2°C, current density of 10 A/dm^2 and a run time of 8 h. Steel strips (DIN - R St 37-2) were used as anodes. Afterwards two of the samples were vacuum annealed for 1h under a pressure of 200 Pa at 600°C and 950°C.

Table 1. Chemical composition of Armco and electrolytic iron (wt %)

Element	C, %	Si, %	Mn, %	Cr, %	Mo, %	Ni, %	Co, %	Cu, %	P, %	S, %	Fe, %
Armco Fe	0,020	0,130	0,139	0,033	0,002	0,073	0,008	0,090	0,007	0,020	Bal.
Electrolytic Fe	0,000	0,015	0,003	0,004	0,002	0,028	0,015	0,040	0,006	0,002	Bal.

The vacuum ONC was carried out in industrial equipment for 7 hours at 550°C in NH_3 and CO_2 atmosphere. The pressure in the vacuum chamber has been 8.10^4 Pa for the first 5 hours and 1.10^5 Pa during the last 2 hours [4]. The surface hardness is measured by a mobile 'Krautkramer' Vickers tester (before and after the ONC) under a load of 1 kg. The microhardness is measured under a load of 0,05 kg according to a chess-board order 4…5 times for each sample. The microstructure was etched by 4%-solution of HNO_3 in ethyl alcohol (Nital) and Murakami reagent. X-ray diffractometer URD 6 using FeKα radiation was used to determine the phase composition. ε-Fe_3(N,C) lattice parameters were determined according to [5]. The structural characteristics before and after modification of the layers were investigated using Olympus BX41M optical microscopy.

3. Results and Discussions

3.1 Microstructure

Fig. 1 displays the microstructures of founded A-Fe, E-Fe and vacuum annealed E-Fe at 600°C and 950°C respectively. The A-Fe ferrite microstructure with Fe_3C at the grains' boundaries and rarely in the grains (fig.1a) is comparatively coarse (average 20 μm grain size). Unlike, the E-Fe (fig.1b) has an entirely different structure and properties. The E-Fe is obtained at a low density asymmetric current in the bath. At this condition, the ferrite nuclei are small because of the lower Fe-ions' mobility in low voltage. The supply ions rate is lower than the ferrite nuclei growth. As a result the density current is redistributed over nuclei-free areas. In restrain growth conditions, oxygen and other surface active components passivate the nuclei. Ions such as Cu, Ni, Mn from the anodes and hydroxides from the solution also incorporate in the nuclei, thus increases the surface strain which is a precondition for development of micro- and submicrocracks. So, the coating presents porous and tense aggregates of small, slightly bounded crystals which mounted perpendicularly to the substrate thus decreasing the surface free energy of the growing up layer.

The vacuum annealed E-Fe at 600°C (fig.1c) contains re-crystallized ferrite grains located predominantly near to the surface where the microstrains of the ultra fine grains are higher. The fully vacuum annealed E-Fe structure (fig.1d) shows that coarse ferrite grains substitute the ultra fine structure. Globular fine phases of oxides are present in the α-Fe grains.

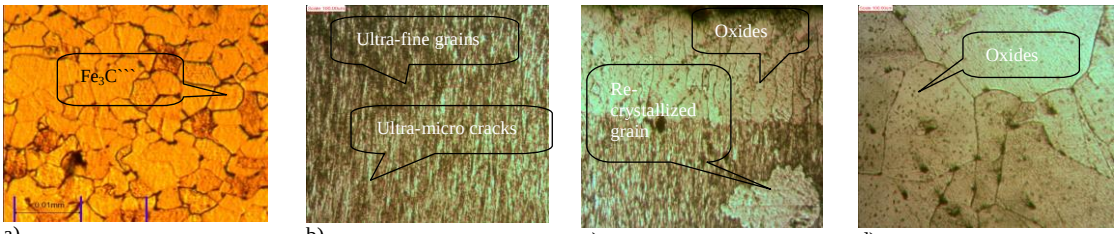

a) b) c) d)

Fig.1 Microstructure images of the iron before ONC etched in Nital: a) A-Fe (200x); b) untreated E-Fe (500x); c) vacuum annealed at 600°C E-Fe (500x); d) vacuum annealed at 950°C E-Fe (500x).

Fig.2 represents the microstructure of the ONC-ed layers formed on the different substrates. The distances of N and C diffusion in ultra fine grained Fe are less than that in the annealed samples as seen on fig.2a. The gas-solid interaction rate depends on the adsorption rate and the latter has a constant quantity at a constant temperature. The nascent atoms retard the diffusion rate when they reach up the substrate grains. The diffusion there runs across the α-Fe grains and the boundaries. The Armco γ'-Fe_4N needles are coarse and consolidated deeper in the substrate. Darker colored $Fe_3(N,C)$ are seen mainly near to the surface, at the grater microcarcks and the electrolyte-Armco Fe boundary. The initial C enrichment precedes compound layer formation during gas nitrocarburizing of Fe and steel [6]. As a smaller molecule, CO_2 is absorbed through the pores of the layer. A carbon concentration gradient in depth probably renders the N penetration because C increases the nitrogen activity. This fact corresponds with the slower rate of compound layer formation. The latter seems comparatively thin and torn to pieces. The faster diffusion in the E-Fe renders surface limited concentration for dense compound layer formation. At the same time, N and C nascent atoms gather the electrolyte-Armco Fe boundary where a secondary adjacent compound layer could be formed [7,8]. Some recrystallized α grains are present in the E-Fe layer after ONC, whereas they are absent before the saturation. A possible reason for this is the formation of $Fe_\alpha(N)$ or $Fe_\alpha(N,C)$. Hence the process time and temperature are enough for primary recrystallization to begin especially in microstrained zones.

Carbon enriched areas in vacuum annealed at 600°C E-Fe (fig.2b) are closely adjacent to the compound layer where carbonitrides in the recrystallized grains are very fine. The compound layer is thicker than in the untreated ONC-ed E-Fe and there is less γ'- needles in the substrate. The recrystallized dendrite-shaped upper ferrite layer retards the diffusion of the nascent atoms and their penentrance is cramped. In spite of that there are compound layer nuclei in the non-recrystallized areas of the E-Fe like that in the untreated ONC-ed E-Fe.

The ONC-ed structure of the vacuum annealed at 950°C E-Fe and bulk A-Fe (fig.2c,d) shows differently shaped, sized and distributed nitrides. The finest needle-shaped nitrides in the E-Fe probably are α"-precipitates [9]. The α"-crystal structure represents eight body-centred tetragonal lattices (Fe_8N or $Fe_{16}N_2$). The latter formation is facilitated due to the lattice resemblance. The α"-nitrides contain less N atoms than γ'-ones. That's why α"-precipitates are centred in the E-Fe grains where the N concentration is less than at the boundaries. Consolidated γ'-Fe_4N are evident not only at the boundaries and near the surface but at the electrolyte-Armco Fe boundary where the nitrides coalesce because of the intensive N

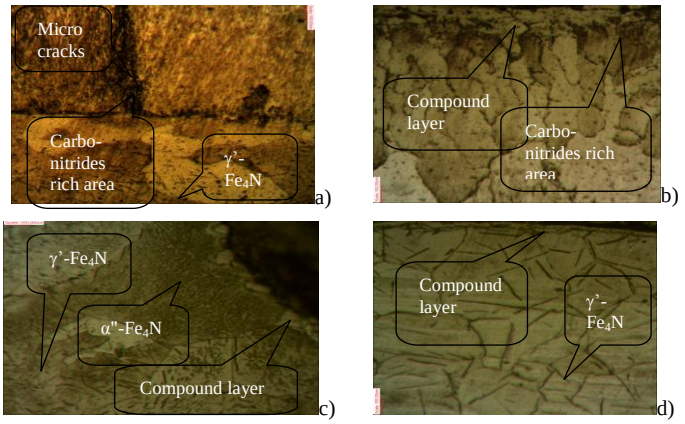

Fig.2 Microstructure images of the ONC-ed iron samples etched with Nital and Murakami reagent (500x): a) untreated E-Fe; b) vacuum annealed at 600°C E-Fe; c) vacuum annealed at 950°C E-Fe; d) vacuum annealed at 950°C A-Fe.

diffusion [10] and the defective structure. The surface orientation of the Armco grains (fig.2d) affects the γ'-Fe_4N growth. In this substrate γ'-nitrides development depends mainly on the N diffusion in the α-grains. Fe_4N grows up in {210} orientated grains in <100> direction [11]. During full annealing and ONC the α-grains release the excess C in form of boundary located Fe_3C. As the C concentration in α-Fe increases the N activity and thus decreases its solubility in the ferrite [3], this could be the reason for less nitride needles in Armco than in the fully annealed E-Fe. Consequently, the higher N and C surface concentration and the Fe_3C presence enhance a dense and integral compound layer formation. The spectral analysis shows a carbon concentration increase at an average of 0,035 % in 0,1 mm depth.

3.2 XRD analysis for the non- and heat treated and oxy-nitrocarburized samples.

It is found that the traces of C, Mn, Si, Ni, etc. in the untreated A-Fe and the oxides and other solid solutions in the vacuum annealed E-Fe don't substantially change the α-Fe lattice parameters because there is a coincidence of the three α-phase diffraction peaks. The untreated E-Fe peaks are shifted and as a result, there is a total coincidence of the theoretical and experimental α-Fe parameters. There is symmetrically widening of the latter peaks which means fine grained and strained structure [12].

Fig.3 compares the X-ray diffraction patterns of the ONC-ed samples. The quantity of γ'- is more than ε-phase in the untreated ONC-ed E-Fe (fig.3a). From thermodynamic point of view the Gibbs free energy for ultra fine grained material at 500°C is -8,22 kJ/mol for γ'- and -1,69 κJ/mol for ε-phase formation. A grate part of free energy is locked in this strained structure in form of non-equilibrium defects that also push ahead the γ'-phase transformation. The extent of the phase transformation depends on the grain size distribution [13]. As the fine grains predominate the quantity of the γ'-phase is greater. The activating energy for N diffusion through the boundaries is approximately half in comparison with crystal lattice diffusion [14]. An approval of the ε-phase carbo-nitride character is the decrease in c/a lattice parameters [15]. There is such a decrease in all of the treated samples but the calculated one is scarcely perceptible probably due to the low carbon potential in the gas phase. According to [16] the gas phase carbon potential should be high enough when Fe and low-carbon steels were nitrocarburized. The content of ε-phase in the low temperature annealed E-Fe (fig.3b) is higher than that shown in fig.4a. In steels ε-Fe_3(N,C) forms easily from Fe_3C [17]. The ε-phase here is a result of a continuous increase in the surface N concentration and retard diffusion through the recrystallized grains. The X-ray diffraction pattern of the vacuum annealed at 950 °C E-Fe (fig.3c) and A-Fe (fig.3d) shows γ'-nitride prevalence in both of them. In the A-Fe sample except due to the continuous increase in the surface nitrogen concentration, Fe_3(N,C) phase may be formed by means of Fe_3C transformation. The spectral analysis shows a carbon concentration increase at an average of 0,027% at the surface of the ONC-ed A-Fe.

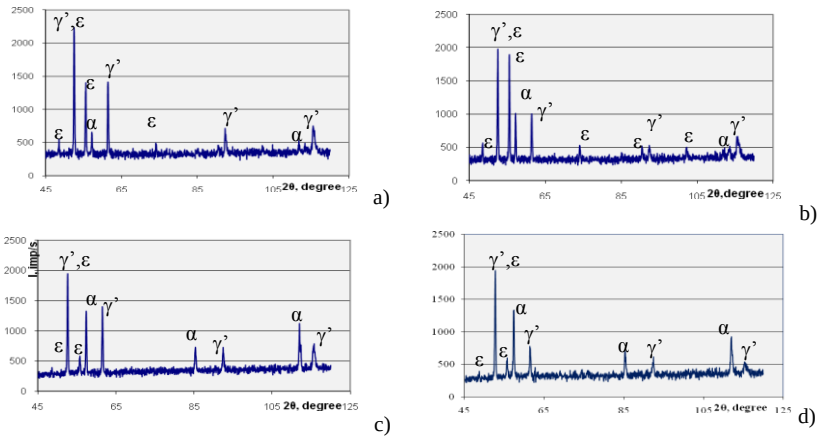

Fig.3 XRD pattern of ONC-ed samples: a) untreated E-Fe; b) vacuum annealed at 600°C E-Fe; c) vacuum annealed at 950°C E-Fe; d) annealed at 950 °C A-Fe.

As a result of the uneven nitrides distribution in the tree possible directions, a tetragonal distortion of α-phase occurs. The extension of some diffraction peaks probably corresponds with the strain field anisotropic character around the nitride precipitates and their predominant crystallographic orientation in the α-Fe matrix [12].

3.3 Cross-sectional hardness profile

The hardness of the diffusive layer (table 2) should be associated with the pre-saturation of the α-solution, nitrides' precipitation, compressive residual stress [18,19] and the initial hardness of the substrate. As it could be expected, the increase in the hardness is not great because it is due to the fine but soft phases or reside stress in the structure. The vacuum annealed at 950 °C E-Fe (fig.4c) and A-Fe (fig.4d) shows a gradual microhardness decrease. The fully annealed E-Fe microhardness remains slightly higher than the A-Fe one because of the smaller nitride phases. The pre-saturation of the α-Fe and the low compressive stress determine the increase in the A-Fe hardness. The microhardness of the vacuum annealed at 600°C E-Fe at a distance of 150 μm from the compound zone towards the core slightly decrease and then maintains unchanged (fig.4b).This surface values correspond to the dendrite-like recrystallized grains. The underneath increase (150 - 250 μm) of the hardness conform to the ultra fine, strained and nitrogen rich electrolytic zone. The highest microhardness value belongs to the untreated ONC-ed E-Fe (fig.4a). The fluctuation in the measurements is due to the partial relaxation of the III^{-rd} type structural stresses and the recrystallization near to the surface as well as the nitrogen saturation in depth. The lack of coincidence in the maximum values of the untreated and annealed at 600°C Fe is due to the difference in E-Fe thickness and the position of the recrystallized boundary in them.

Table 2. Hardness values (HV_1) before and after oxy-nitrocarburizing.

Sample		Untreated [HV_1]	600°C annealed [HV_1]	950°C annealed [HV_1]
Before ONC	E-Fe	400	80	75
	A-Fe	130	125	120
After ONC	E-Fe	550	350	235
	A-Fe	-	-	205

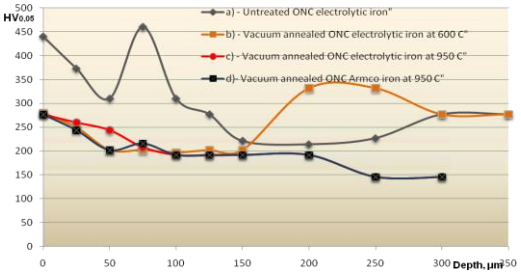

Fig.4 Comparison of the depth profile of the microhardness results of the vacuum ONC-ed E-Fe and A-Fe without and after vacuum annealing.

4. Conclusion

The main conclusions from this investigation could be summarized as followed:
1. The structural characteristics of the substrate determine to a great extend the diffusion rate and the saturation depth of the vacuum oxy-nitrocarburized layers.
2. According to the metallographic analysis, the carbon enriched areas appears in the oxy-nitrocarburized samples near the surface, in some defective regions in the electrolytic Fe and in the electrolyte-Armco Fe boundary where the nascent atoms decrease their diffusion rate. The diffusion of N is many times greater than the C one. In the oxy-nitrocarburized Armco Fe, the increased C content at a distance of 0,1 mm is due to C diffusion in the substrate.
3. It is found out that the ε-phase C-content is comparatively low in the indicated process conditions.
4. The essential structural differences in the fully annealed electrolytic and Armco Fe compound and diffusion layer are shown. While the electrolytic Fe saturated zone contains a thinner ε- and γ'-built compound layer and α" and γ'- constructed diffusion layer, the Armco Fe shows a comparatively dense ε- and γ'-built compound layer and coarse γ'-nitride precipitates in the diffusion layer.
5. There is an inconsiderable hardness increase after treatment due to the pre-saturation of the α-Fe and compressive stress in the Armco substrate. The quantity and the dispersion of the nitride phases in the annealed samples contribute to the hardness rise. In the untreated and low temperature annealed oxy-nitrocarburized samples there is an additional strength because of the residual stress in the structure.

Acknowledgements

The study was supported by contract № BG051PO001-3.3.04/28, "Support for the Scientific Staff Development in the Field of Engineering Research and Innovation". The project is funded with support from the Operational Programme "Human Resources Development" 2007-2013, financed by the European Social Fund of the European Union.

References

[1] Bell T., Heat Treat. Met., 1975, 2(2), p.39–49;
[2] Dawes C., Tranter DF, Reynoldson RW ., Heattreatment'73; London, The Metals Society; 1973;
[3] Winter Karl-Michael, Techn. Paper, Process-Electronic GmbH, United Process Controls, Heiningen, Germany;
[4] Danev P., Ruse-University Scientific Proceedings, Ruse, 2004, p. 73-77, ISSN 1311-3321;
[5] Горелик СС., Расторгуев ЛН., Скаков ЮА., Металлургия, Москва 1970, 4;
[6] Naumann FK., Langenscheid G., Arch. Eisenhuttenwes. 36, 1965, p.583-590;
[7] Nikolova M, Danev P., Dermendjiev I, Metal 2010, 19 Int. Metal. Conference: Roznov pod Radhostem, May 2010, p 148;
[8] Somers M. Proefschrift; Chem. Tech. and Mat. Sci. of the Delft University of Technology, 1989;
[9] Maliska AM, de Oliveira AM., Klein AN, Muzart JLR, Surf . Coat. Technol., 141 (2001) 128-134;
[10] Каратеев АМ., Павлюченко АА., Костик ЕА., Вост. – европейский Журнал Передовых Технологий – 4/1(16), 2005;
[11] Bernal JL., Salas O., Figueroa U., Oseguera J., Surf. Coat. Technol. 177-178 (2004) p.665-670;
[12] Jung KS., Schacherl RE., Bischoff E., Mitemeijer EJ., Surf. Caot. Technol. 204 (2010) 1942-1946;
[13] Pelka R., Arabczyk W., 2nd National Conference on Nanotechnology, NANO 2008;
[14] Tong WP., Tao NR., Wang ZB., Lu J., Lu K., Sci, Vol 299, 203;
[15] Naumann FK, Langenscheid, G. Arch Eisenhüttenw 1965; 36:677;
[16] http://www.eltromoscau.narod.ru/karbon_oxid.htm;
[17] Ratajski J., Surf Coat. Technol. 203 (2009);
[18] Bell T., Loh NI., Heat Treatment, 2, (1982) 232;
[19] Priestner R., Priestner DM, Surf. Eng. 10 (1994) 65.